Sixth International Conference on Durability of Concrete Structures
18 - 20 July 2018
University of Leeds, Leeds, West Yorkshire, LS2 9JT, United Kingdom

Paper Number ICC17

Post-Cracking Behavior of Cementitious Composite Incorporating Nano-Silica and Basalt Fiber Pellets

A.G. Bediwy, M.T. Bassuoni and E. El-Salakawy
Civil Engineering, University of Manitoba, Winnipeg, Canada

ABSTRACT

Recently, fiber reinforced polymers (FRPs) have been increasingly used to reinforce concrete structures in harsh environments, due to their non-corrodible nature. Developing a nonferrous reinforcement system (corrosion-free system) for concrete using FRP bars along with discrete fibers is a promising option for exposed concrete structures in cold regions or marine environments. Incorporating highly efficient non-metallic fibers into any cementitious composite is capable of reducing bleeding, controlling shrinkage cracking, and improving toughness and impact resistance. Therefore, in this study, a new type of basalt fiber pellets with high tensile strength was investigated. This paper reports on the flexural performance of the basalt fiber-reinforced cementitious composite (BFRCC) compared to steel fiber-reinforced cementitious composite (SFRCC). The cementitious composite incorporated general use cement, slag and nano-silica. The key mechanical property determined was the post-cracking behavior in terms of residual strength, and toughness. Standard prisms (100 × 100 × 350 mm) were cast using basalt fiber pellets and steel fibers with three different dosages and tested after 28 days following the general guidelines of ASTM C1609 (Standard Test Method for Flexural Performance of Fiber-Reinforced Concrete). Analysis of results showed a high level of effectiveness of the basalt fibers to enhance the post-cracking behavior of specimens, as they behaved comparably or superiorly (first cracking, load-deflection relationship, and toughness) to counterpart specimens comprising steel fibers.

Keywords: Basalt Fibers, Steel Fibers, Cementitious Composites, Post-Cracking, Pseudo Strain Hardening.

1.0 INTRODUCTION

Concrete often cracks due to its limited tensile strength and deformational capacity. The presence of cracks may not only affect the aesthetics of structures, but also their durability by allowing infiltration of moisture and oxygen causing corrosion of reinforcing steel accompanied by deterioration of concrete (Vasanelli *et al*., 2013). In addition, the presence of de-icing salts and repeated freezing-thawing cycles, particularly in cold regions, will aggravate the damage of concrete. Thus, in order to expand the possibilities of using concrete in such harsh environments, developing high performance mortar/composite and concrete to rehabilitate concrete infrastructure facilities (e.g. bridge decks, pavements, parking structures) is much needed (Nes and Øverli, 2015). In this context, the use of fiber reinforced concrete (FRC) has been explored by many researchers to enhance the short-term structural performance. Incorporating discrete fibers into any cementitious composite is capable of reducing bleeding, controlling shrinkage cracking, and improving impact resistance. Furthermore, the most pronounced advantages of using fibers in cementitious composites are increasing their energy absorbing capacity/toughness, deformation capability, and load bearing capacity after cracking (Bentur and Mindess, 2007).

Various commercially available fibers can be used to make fiber reinforced cementitious composite (FRCC), such as steel, synthetic and organic or inorganic fibers. However, a relatively new type of fibers manufactured from basalt rocks is progressively immerging in civil engineering research, including a special type called basalt fiber pellets [BF], which is made of basalt fibers encapsulated by polyamide or other resins. The production process of basalt fibers is more environment-friendly, and it is cheaper with respect to the other types of fibers such as glass fibers. Also, basalt fibers have high tensile strength, and they are not vulnerable to corrosion contrary to the case of steel fibers that corrode resulting in irregular/rough surfaces, e.g. slab on ground, bridge decks and pavements (Iyer *et al*., 2015; Arslan, 2016; Iyer *et al*., 2016; Ayub *et al*., 2016; Ghazy *et al*., 2016a; Mahmoud *et al*., 2017).

Despite the advantages of fibers, it was reported that adding fibers in mortar/concrete may increase its permeability due to the formation of numerous weak interfacial transition zones (ITZ) between the fibers and cementitious matrix. In addition, the efficacy of fiber reinforcement depends upon the matrix composition (Bentur and Mindess, 2007; Banthia *et al*., 2014; Soylev and Ozturan, 2014; Zheng *et al*., 2015; Afroughsabet and Ozbakkaloglu, 2015; Ghazy *et al*., 2016). Therefore, producing a cementitious composite with high performance properties is crucial which can be obtained by incorporating supplementary cementitious materials (SCMs) such as silica fume and/or ground granulated blast-furnace slag. Nevertheless, it is worth noting that slag is a latent hydraulic binder, as incorporating high dosages of slag usually leads to delay of hardening and strength as well as microstructural development at early ages (Malhotra *et al*., 2000; Zhang *et al*., 2012). It is well-documented that adding a small dosage of innovative materials such as nanoparticles (e.g. nano-silica, NS) can vigorously speed up the kinetics of cement hydration, especially at early ages, besides the contribution to the microstructural development of cement-based materials (Said *et al*., 2012; Zhang *et al*., 2012; Kong *et al*., 2012; Madani *et al*., 2012; Ghazy *et al*., 2016b). Thus, nanoparticles can mitigate the early-age shortcomings of slag and fly ash, when incorporated in mortar/concrete (Ghazy *et al*, 2016).

The main objective of this study was to investigate the behavior of high-strength nano-modified cementitious composites incorporating 40% slag and reinforced with discrete BF pellets (coated BF). The effect of varying basalt fiber pellets dosages on the compressive strength, flexural strength, and toughness of these composites was evaluated. In addition, for comparison purposes, the performance of steel fiber reinforced cementitious composite (SFRCC) was also evaluated.

2.0 Experimental Program

2.1 Materials

General use (GU) cement and slag, which meet the requirements of CSA-A3001 standard (CSA, 2013), are used as the main components of the binder. The chemical and physical properties of these main components are shown in Table 1. In addition, a commercial nano-silica (NS) sol (50% solid content of SiO_2 particles dispersed in an aqueous solution) was incorporated in the binder. The mean particle size of the Ns was 35 nm, and the specific surface, viscosity, density and pH values were 80 m^2/g, 8 cP, 1.1 g/cm^3 and 9.5, respectively. Locally available fine aggregate, with a fineness modulus of 2.9 and a gradation of 0 to 600 μm, was used to prepare the mixtures. The specific gravity and absorption of the fine aggregate were 2.6 and 1.5%, respectively. A high-range water-reducing admixture (HRWRA) based on polycarboxylic acid and complying with ASTM C494 Type F (ASTM, 2013) was added to maintain a comparable target flow of 150±15 mm for all the mortar mixtures according to ASTM C230 (ASTM 2014). The cementitious composites were reinforced with either BF pellets or steel fibers [Figs. 1(a)-(b)]. The BF pellets were made of 16-micron basalt roving encapsulated by polyamide resin, and the BF represented 60% of the pellet by mass. The BF pellets were 36 mm long with a diameter of 1.8 mm. Hooked-end steel fibers of 0.5 mm diameter and 30 mm length were also used. The properties of the BF pellets and the steel fibers are listed in Table 2.

Table 1. Chemical and physical properties of GU cement and slag

Binder	Chemical composition (%)					Physical properties	
	SiO_2	Al_2O_3	Fe_2O_3	CaO	MgO	Blaine (m^2/kg)	Specific Gravity
Cement	19.2	5.01	2.33	63.2	3.31	390	3.15
Slag	33.4	13.4	0.76	42.7	5.3	492	2.87

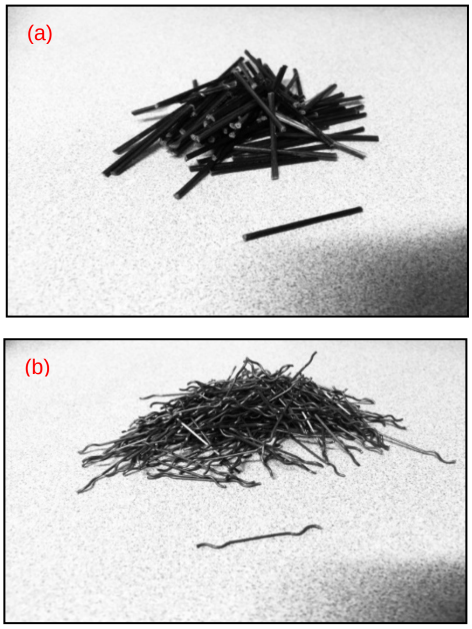

Fig. 1. Reinforcing fibers: (a) BF pellets, and (b) steel fibers

Table 2. Properties of fibers

	BF pellets	Hooked steel
Length (mm)	36	30
Diameter (mm)	1.8	0.65
Aspect ratio	20	45
Specific gravity	1.74	7.7
Tensile strength (MPa)	2300	1200
Elastic modulus (GPa)	65	200

2.2 Proportions and Mixing Procedures

A total of seven mixtures were prepared with GU cement and a constant dosage of slag (280 kg/m^3), representing 40% replacement by mass of binder (700 kg/m^3 comprising GU cement and slag), and the NS was added at a dosage of 6% by mass of binder. The water-to-binder ratio (w/b) was kept constant at 0.30 for all mixtures. Six mixtures were reinforced with BF pellets and steel fibers. The dosages of the

BF pellets and steel fibers were selected based on keeping either the volume of the fibers or the ratio of volume of BF pellets to steel fibers equal to the modular ratio (the ratio of modulus of elasticity of steel fibers to that of BF pellets).The BF pellets were added to the mixtures at dosages of 2.5%, 4.5% and 6.9 % by volume, equivalent to 1%, 1.85% and 2.75% of basalt fibers by volume of composite fiber, whereas in the case of steel fibers, the respective dosages were 0.4%, 0.7%, and 1% by volume. The proportions of all cementitious composite mixtures are listed in Table 3. For the mixture coding, the first letter refers to the fiber type ("B" for basalt fiber pellet and "S" for steel fiber). The second number represents the fiber dosage percentage used. The mixing procedures introduced by Mahmoud *et al*., (2017) was followed herein, except for the timing of adding the fibers, as it was incorporated after adding the liquid phase to the mixture to alleviate the foaming action. Detailed discussion of the mixing sequence was given in the previous study (Mahmoud *et al*., 2017).

Table 3. Proportions of the mixtures per cubic meter

Mixture ID	Cement (Kg)	Slag (Kg)	Water[a] (Kg)	Nano-silica (Kg)	Fine aggregate (Kg)	Fibers (Kg)	
						BF pellets	Hooked steel
Ref	420	280	180	84	1,328	-	-
B-2.5	420	280	180	84	1,263	43.3	-
B-4.5	420	280	180	84	1,208	80.5	-
B-6.9	420	280	180	84	1,150	119.2	-
S-0.4	420	280	210	84	1,318	-	28.1
S-0.7	420	280	180	84	1,310	-	52.4
S-1.0	420	280	180	84	1,302	-	77

[a] Adjusted amount of mixing water considering the water content of nano-silica.

2.3 Tests

To determine the compressive strength of the mixtures, triplicate cylinders (100×200 mm) were tested at 28 days according to ASTM C39 (ASTM, 2012a). This test method is used to apply a compressive axial load to molded cylinders at a rate ranging from 0.15 to 0.35 MPa/s, until failure occurs. Following the guidelines of ASTM C1609 (ASTM, 2012b), a four-point bending test was carried out at 28 days to evaluate the flexural performance of the mixtures using three standard prisms (100×100×350 mm). A closed-loop, servo-controlled testing machine was used to apply the load, where the loading rate was governed by the measured net mid-span deflection of the beam, as shown in Fig. 2. The residual strength at net deflection of (span/600) and (span/150) was calculated based on the following equation:

$$f = \frac{PL}{bd^2} \tag{1}$$

where, f is the strength (MPa), P is the load (N), L is the span length (mm), b is the average width of the specimen at the fracture, as oriented for testing (mm), and d is the average depth of the specimen at the fracture, as oriented for testing (mm). Moreover, the flexural toughness is commonly defined as the area under the load-deflection curve (P-δ), and it is also referred to as the total energy to fracture (Bentur and Mindess, 2007). However, in this study, the toughness was calculated according to ASTM C1609 (ASTM, 2012b) as the area under the P-δ curve up to a deflection of span/150 (2 mm for the tested prisms).

Fig. 2. Flexural test set-up

3.0 Results and Discussion

3.1 Compressive strength

The average compressive strengths of Ref., BFRCC and SFRCC, obtained from cylinders, are listed in Table 4. Compared to the control/reference mixture without fibers, BFRCC and SFRCC with fibers showed lower compressive strengths. A similar trend was obtained by Branston *et al*. (2016) and Olivito and Zuccarello (2010) for BF mini bars and steel fibers, respectively. Furthermore, the failure mode was considerably altered from fragile/sudden to ductile/confined, as the bridging effect of the fibers maintained the integrity of the cylinders up to the end of the test, as depicted in Fig. 3. The results were assessed by the analysis of variance (ANOVA) to determine whether there are any statistically significant differences between the means of compressive strength, as shown in Table 5. According to Montgomery (2012), exceeding the F_{cr} value of an F distribution density function indicates that the variable tested has a significant effect on the average results.

Table 4. Compressive and flexural test results at 28 days

Mixture ID	Compressive strength (MPa)	Flexural test results			
		First-peak strength (MPa)	Residual strength at L/600 (MPa)	Residual strength at L/150 (MPa)	Toughness (J)
Ref	87.4	8.6	-	-	0.9[a]
B-2.5	80.8	7.6	4.9	4.1	32.1
B-4.5	70.1	6.4	8.6	7.7	54.9
B-6.9	63.7	5.8	8.8	7.9	56.5
S-0.4	72.3	7.3	3.1	2.4	20.7
S-0.7	79.8	7.1	4.4	3.1	26.1
S-1.0	85.8	7.6	5.2	3.7	31.4

[a]Toughness calculated as the area under the *P-δ* curve from 0 to the peak load deflection
Note: *L* is the span of the test specimen = 300 mm

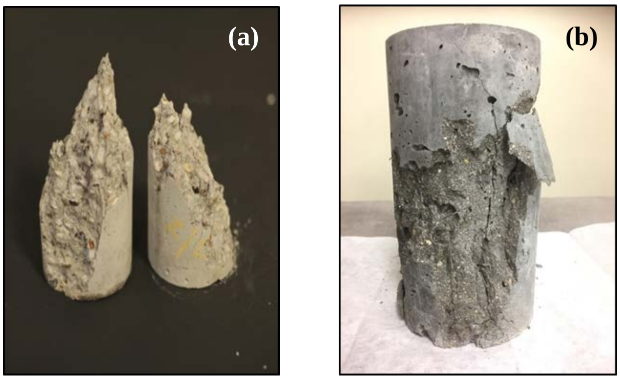

Fig. 3. Mode of failure of specimens: (a) without fibers, and (b) with fiber

The ANOVA showed that incorporating the BF pellets in the matrix yielded *F* value of 14.5, which was higher than the critical value (F_{cr}) of 4.1, indicating that the effect of adding such fibers on the compressive strength was statistically significant. For example, the compressive strength was markedly reduced by 14 and 22% when the composite was reinforced with BF pellets at dosages of 4.5 and 6.9%, respectively. This may be attributed to the formation of additional interfacial transitional zones (ITZs) in the matrix, and entrapment of air bubbles in the cementitious matrix, as previously observed by Mahmoud *et al*. (2017). This trend was statistically substantiated by the ANOVA results, as increasing the dosage of BF pellets from 2.5 % to 6.9% had *F* value of 7.7 compared to F_{cr} of 5.1.

Unlike the BF pellets, the incorporation of steel fibers had insignificant effect on the compressive strength with respect to the control mixture. This was statistically supported by ANOVA for the compressive strength results, as adding steel fibers, regardless of the dosage, yielded *F* value of 3.1, which was less than the F_{cr} of 4.1. This insignificant effect might be ascribed to the small volumes of steel fibers introduced to the cementitious matrix, as the highest dosage in the steel fiber mixtures corresponded to the lowest dosage in the BF pellet mixtures. Although varying the dosage of steel fibers from 0.4% to 1.0% led to 15% increase in the compressive strength value, the ANOVA results revealed insignificant differences among the compressive strength results for the mixtures incorporating different dosages of steel fibers. For instance, increasing the dosage of steel fibers from 0.4% to 1.0 % had *F* value of 2.4 compared to F_{cr} of 5.1.

It is worth noting that the compressive strength was marginally affected by the properties of fibers. The incorporation of fibers, regardless of the fiber type, usually contributes to increasing air bubbles in the matrix, and thus reducing its strength (Salemi and Behfarnia, 2013). This was confirmed by ANOVA for the compressive strength results, as replacing the BF pellets with steel fibers yielded *F* value of 3.5 which is smaller than the F_{cr} value of 4.5 (Table 5), highlighting the predominant role of the cementitious matrix in significantly reducing/increasing the compressive strength, rather than the type of fiber (BF pellets or steel fiber). In addition, when the volume was kept constant, the same observation was found. As replacing 2.5 % of BF pellets with 1% steel fiber yielded *F* value of 3.4, which is less than the F_{cr} value of 7. Thus, it can be concluded that the variability of compressive strength within the two groups (BF pellets and steel fibers) was quite comparable.

3.2 Flexural strength and toughness

The flexural strength and toughness for all mixtures are listed in Table 4. In general, the fibers had marginal effect on the behavior during the pre-cracking stage which was mainly dependent on the properties of cementitious matrix. The first-crack strength (first-peak strength) for some fiber reinforced composites (B-2.5, S-0.4, S-0.7, S-1.0) with either pellets or steel fibers, showed comparable values with respect to the control mixture without fibers. Comparatively, the mixtures comprising high dosages of BF pellets at 4.5 and 6.9% showed lower flexural strength conforming to the preceding results of compressive strength. This trend was statistically substantiated by the ANOVA results, as incorporating the BF pellets in the matrix yielded *F* value of 30.4, which was higher than the critical value (F_{cr}) of 4.1, indicating that the effect of adding such fibers on the first-crack strength was statistically significant due to the their effects on the cementitious matrix, as discussed earlier. Adding steel fibers to the matrix did not significantly affect the first-crack strength due to the lower dosages of steel fibers added, as varying the dosages of steel fibers from 0.4 % to 1.0% had *F* value of 0.2, which was much lower than F_{cr} of 9.6, indicating the dominant effect of the cementitious matrix on the pre-cracking behavior. Similarly, replacing the BF pellets with steel fibers did not show any distinctive difference in terms of the first-crack strength, even if the modular ratio and the volume

Table 5. ANOVA for the results of compressive strength, flexural strength and toughness at 28 days

	Compressive strength			First-peak flexural strength			Toughness		
Parameter	F	F_{cr}	Effect	F	F_{cr}	Effect	F	F_{cr}	Effect
Effect of the BF pellets									
B-2.5, B-4.5, B-6.9 vs. Ref.	14.5	4.1	Significant	30.4	4.1	Significant	193.6	4.1	Significant
Effect of the dosage of BF pellets									
B-2.5 vs B-6.9	7.7	5.1	Significant	12.7	5.1	Significant	40.2	5.1	Significant
Effect of steel fibers									
S-0.4, S-0.7, S-1.0 vs. Ref.	3.1	4.1	Insignificant	3.6	5.4	Insignificant	84.1	5.4	Significant
Effect of the dosage of steel fibers									
S-0.4 vs S-1.0	2.4	5.1	Insignificant	0.2	9.6	Insignificant	6.3	9.6	Insignificant
Effect of BF pellets vs. steel fibers (constant modular ratio)									
B-2.5, B-4.5, B-6.9 vs S-0.4, S-0.7, S-1.0	3.5	4.5	Insignificant	3.2	4.7	Insignificant	16.4	4.7	Significant
Effect of BF pellets vs. steel fibers (constant volume)									
B-2.5 vs S-1.0	3.4	7.7	Insignificant	.01	10.2	Insignificant	0.25	10.2	Significant

were kept constant; such insignificant effect was also validated by the ANOVA results (see Table 5).

The P-δ curves for all test prisms are shown in Fig. 4. The reported mid-span deflection represents the average readings from two LVDTs that were in contact with a bracket attached to each specimen. As expected, the prism made without any fibers did not show any residual strength after cracking and broke in a brittle manner, whereas all FRCC prisms, irrespective of the type of fibers added to the mixture, exhibited improved post-cracking behavior due to deformation and pullout mechanisms of the BF pellets and the steel fibers.

After first cracking, the prisms did not fail but it continued to carry either decreasing loads (B-2.5, S-0.4, S-0.7, and S1.0) or increasing loads (B-4.5 or 6.9). The post-cracking behavior of the former prisms was associated with a sudden drop (an average of 53% at approximately 0.25 mm deflection) in the load; however, the fiber in these prisms were able to control the crack exhibiting a notable increase in composite fracture resistance which was accompanied by a slight increase in load carrying capacity. As for the later prisms, no drop in the load was observed, but it continued to carry increasing loads, whereas the peak load of the composite was notably greater than that of the load at first-cracking. The prisms reinforced with high dosages of BF pellets (B-4.5 and B-6.9) exhibited a pseudo strain hardening behavior, similar to Engineered Cementitious Composites which nearly behave as ductile metals (Li and Leung, 1992). The prisms from B-4.5 and B-6.9 achieved the highest post-cracking behavior, as the residual strengths at a deflection of 0.5 mm (span/600) were

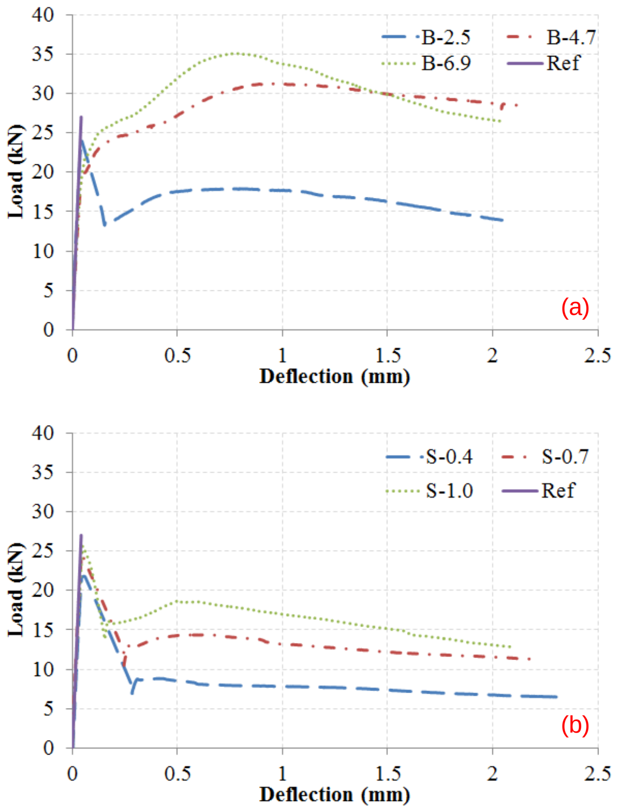

Fig. 4. Load-deflection (P-δ) curves for: (a) BF pellets fibers, and (b) steel fibers

approximately 135 and 150% of the first-crack strength of both mixtures, respectively. At a deflection of 2 mm (span/150), these percentages were approximately 120 and 136% for both mixtures, respectively. Such distinctive behavior beyond first cracking for both mixtures (B-4.5 and B-6.9) substantiates the well-documented notion that effective types of fibers are mainly incorporated to significantly enhance the flexural (Bentur and Mindess, 2007). This trend might be attributed to the adequate distribution of BF pellets over the cross section of prisms or the intensity of fibers which improved their effectiveness in controlling crack propagation in the matrix by redistributing micro-cracks (Fig. 5) In addition, the improved bonding with the cementitious matrix, resulting in the gradual pull out failure rather than rupture of the pellets, as also observed by Mahmoud *et al*. (2017).

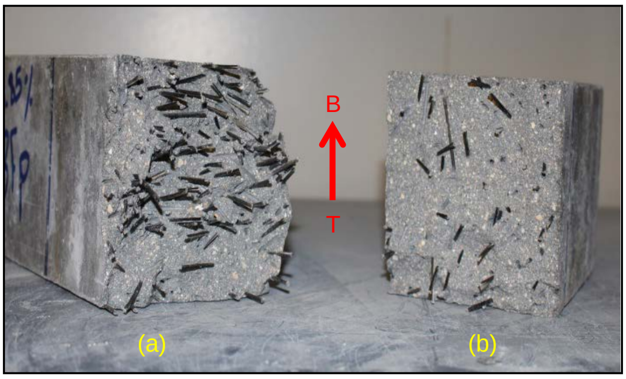

Fig. 5. Distribution of BF pellets at the failure planes of: (a) B-6.9, and (b) B-2.5

Albeit the BF pellets had lower modulus of elasticity and aspect ratio with respect to the steel fibers, a superior post-cracking behavior was observed in terms of residual strength at both deflections (span/600 and span/150) and fracture energy (toughness). In case of keeping the ratio of volume of BF pellets to steel fibers equal to the modular ratio, the toughness was markedly increased. For instance, replacing 1% of steel fibers with 6.9% BF pellets led to a significant increase of 80% in the toughness, which was also confirmed by the ANOVA results (see Table 5). Interestingly, when the volume of both fibers was kept constant, taking into consideration the superior properties of steel fibers with respect to the BF pellets, the post-cracking behavior was quite comparable, as shown in Fig. 6. Accordingly, replacing 2.5 % BF pellets with 1% steel fibers had an insignificant effect on the toughness results. This trend was also substantiated by the ANOVA results, as incorporating the same volume of both types into the matrix yielded F value of 0.25 which was much lower than the critical value (F_{cr}) of 10.2. This may be ascribed to the enhanced bonding of the cementitious composite within the textured grooves of the BF pellets, as reported by Mahmoud *et al*. (2017).

4.0 CONCLUDING REMARKS

In this study, a new type of basalt fiber pellets with high tensile strength was investigated. The flexural performance of the basalt fiber-reinforced cementitious composite (BFRCC) was compared with steel fiber-reinforced cementitious composite (SFRCC). The cementitious composite incorporated general use cement, slag and nano-silica. The key mechanical property determined was the post-cracking behavior in terms of residual strength, and toughness. Standard prisms (100 × 100 × 350 mm) were cast using basalt fiber pellets and steel fibers with three different dosages and tested after 28 days following the general guidelines of ASTM C1609 (Standard Test Method for Flexural Performance of Fiber-Reinforced Concrete). Analysis of results showed a high level of effectiveness of the basalt fibers to enhance the post-cracking behavior of specimens, as they behaved comparably or superiorly (first cracking, load-deflection relationship, and toughness) to counterpart specimens comprising steel fibers.

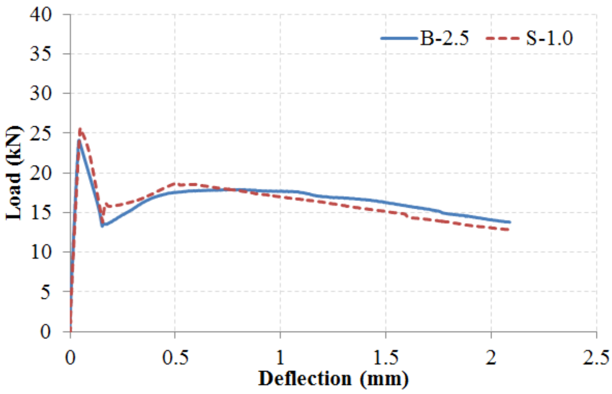

Fig. 6. Load-deflection (*P*-*δ*) curves for B-2.5 and S-1.0

Acknowledgement

The authors highly appreciate the financial support from University of Manitoba Graduate Fellowship. Sponsorship from Sudaglass Fiber Technology, Manitoba Infrastructure, and ACI Manitoba Chapter is much appreciated. The IKO Construction Materials Testing Facility and Heavy Structures Laboratory at the University of Manitoba in which these experiments were conducted have been instrumental to this research.

References

Afroughsabet, V., and Ozbakkaloglu, T., 2015. Mechanical and durability properties of highstrengthconcrete containing steel and polypropylene fibers. Construction and Building Materials, 94: 73–82.

Arslan, M. E., 2016. Effects of basalt and glass chopped fibers addition on fracture energy and mechanical properties of ordinary concrete: CMOD measurement. Construction and Building Materials, 114: 383–391.

ASTM., 2012a. Standard test method for compressive strength of cylindrical concrete specimens. ASTM C39-12, V. 4.02, West Conshohocken, PA.

ASTM., 2012b. Standard test method for flexural performance of fiber- reinforced concrete (using beam with third-point loading). ASTM C1609/C1609M–12, V. 4.02 West Conshohocken, PA.

ASTM., 2013. Standard specification for chemical admixtures for concrete. ASTM C494/C494M-13, West Conshohocken, PA.

ASTM., 2014. Standard specification for flow table for use in tests of hydraulic cement. ASTM C230/C230M-14, West Conshohocken, PA.

Ayub, T., Shafiq, N., and Khan, S., 2016. Compressive stress-strain behavior of HSFRC reinforced with basalt fibers. Journal of Materials in Civil Engineering, ASCE, 28(4): 06015014.

Banthia, N., Zanotti, C., Sappakittipakorn, M. 2014. Sustainable fiber reinforced concrete for repair applications. Construction and Building Materials, 67: 405–412.

Bentur, A., and Mindess, S., 2007. Fiber reinforced cementitious composites, 2nd Ed., E and FN Spon, New York.

Branston, J., Das, S., Kenno, S. Y., and Taylor, C., 2016. “Mechanical behaviour of basalt fibre reinforced concrete. Construction and Building Materials, 124: 878–886.

CSA (Canadian Standards Association), 2013. Cementitious materials for use in concrete. CSA-A3001-13, Mississauga, ON, Canada.

Ghazy, A., Bassuoni, M.T., Maguire, E. and O’Loan, M., 2016a. Properties of fiber-reinforced mortars incorporating nano-silica. Fibers, 4(6): 1-16.

Ghazy, A., Bassuoni, M. T., and Shalaby, A., 2016b. Nano-modified fly ash concrete: A repair option for concrete pavements. ACI Materials Journal, 113(2): 231–242. Iyer, P., Kenno, S. Y., and Das, S., 2015.

Mechanical properties of fiber reinforced concrete made with basalt filament fibers. Journal of Materials in Civil Engineering, ASCE, 27(11): 04015015.

Iyer, P., Kenno, S. Y., and Das, S., 2016. Performance of fiber reinforced concrete made with basalt bundled fibers. Advances in Civil Engineering Materials, 5(1): 107–123.

Kong, D., Xiangfei, D., Wei, S., Zhang, H., Yang, Y., and Shah, S. P., 2012. Influence of nano-silica agglomeration on microstructure and properties of the hardened cement-based materials. Construction and Building Materials, 37: 707–715.

Madani, H., Bagheri, A., and Parhizkar, T., 2012. The pozzolanic reactivity of monodispersed nano-silica hydrosols and their influence on the hydration characteristics of portland cement. Cement and Concrete Research, 42(12): 1563–1570.

Mahmoud, K., Ghazy, A., Bassuoni, M.T., and El-Salakawy, E., 2017. Properties of Nanomodified Fiber-Reinforced Cementitious Composites. Journal of Materials in Civil Engineering, 29(10), 04017173.

Malhotra, V. M., Zhang, M. H., Read, P. H., and Ryell, J., 2000. Long term mechanical properties and durability characteristics of high-strength/ high-performance concrete incorporating supplementary cementing materials under outdoor exposure conditions. ACI Materials Journal, 97(5): 518–525.

Montgomery, D. C., 2014. Design and analysis of experiments, Wiley, New York.

Nes, L. G., and Øverli, J. A., 2015. Structural behaviour of layered beams with fibre-reinforced LWAC and normal density concrete. Materials and Structures, 49(2): 689–703.

Olivito, R.S. and Zuccarello, F.A., 2010. An experimental study on the tensile strength of steel fiber reinforced concrete. *Composites Part B: Engineering*, *41*(3): 246-255.

Said, A. M., Zeidan, M. S., Bassuoni, M. T., and Tian, Y., 2012. Properties of concrete incorporating nano-silica. Construction and Building Materials, 36: 838–844.

Salemi, N. and Behfarnia, K., 2013. Effect of nano-particles on durability of fiber-reinforced concrete pavement. Construction and Building Materials, 48: 934-941

Soylev, T.A., Ozturan, T., 2014. Durability, physical and mechanical properties of fiberreinforced concretes at low-volume fraction. Construction and Building Materials, 73: 67–75.

Vasanelli, E., Micelli, F., Aiello, M. A., and Plizzari, G., 2013. Crack width prediction of FRC beams in short and long term bending condition. Materials and Structures, 47(2): 39–54.

Zhang, M., Islam, J., and Peethamparan, S., 2012. Use of nano-silica to increase early strength and reduce setting time of concretes with high volumes of slag. Cement and Concrete Composites. 34(5): 650–662.

Zheng, X.G., Liu, J., Li, S.M., Zeng, Z., Weng, Z.C., Yang, D.J., 2015. Effect of polypropylene fiber and silica fume on mechanical properties and durability improvement of high performance concrete. Kao, J., Sung, C., and Ren. C. (Eds.), CRC Press, Taylor and Francis Group, London: UK: 333–342.